# Genesis of the South Asian High and Its Impact on the Asian Summer Monsoon Onset

BOQI LIU

*Key Laboratory of Meteorological Disaster of Ministry of Education, Nanjing University of Information Science and Technology, Nanjing, and State Key Laboratory of Numerical Modeling for Atmospheric Sciences and Geophysical Fluid Dynamics (LASG), Institute of Atmospheric Physics, Chinese Academy of Sciences, Beijing, China*

GUOXIONG WU AND JIANGYU MAO

*State Key Laboratory of Numerical Modeling for Atmospheric Sciences and Geophysical Fluid Dynamics (LASG), Institute of Atmospheric Physics, Chinese Academy of Sciences, Beijing, China*

JINHAI HE

*Key Laboratory of Meteorological Disaster of Ministry of Education, Nanjing University of Information Science and Technology, Nanjing, China*

(Manuscript received 17 May 2012, in final form 26 November 2012)

ABSTRACT

The formation of the South Asian high (SAH) in spring and its impacts on the Asian summer monsoon onset are studied using daily 40-yr ECMWF Re-Analysis (ERA-40) data together with a climate-mean composite technique and potential vorticity–diabatic heating (PV–$Q$) analysis. Results demonstrate that, about 2 weeks before the Asian summer monsoon onset, a burst of convection over the southern Philippines produces a negative vorticity source to its north. The SAH in the upper troposphere over the South China Sea is then generated as an atmospheric response to this negative vorticity forcing with the streamline field manifesting a Gill-type pattern. Afterward, the persistent rainfall over the northern Indochinese peninsula causes the SAH to move westward toward the peninsula. Consequently, a trumpet-shaped flow field is formed to its southwest, resulting in divergence pumping and atmospheric ascent just over the southeastern Bay of Bengal (BOB).

Near the surface, as a surface anticyclone is formed over the northern BOB, an SST warm pool is generated in the central–eastern BOB. This, together with SAH pumping, triggers the formation of a monsoon onset vortex (MOV) with strong surface southwesterly developed over the BOB. Enhanced air–sea interaction promotes the further development and northward migration of the MOV. Consequently, the wintertime zonal-orientated subtropical anticyclone belt in the lower troposphere splits, abundant water vapor is transported directly from the BOB to the subtropical continent, and heavy rainfall ensues; the atmospheric circulation changes from winter to summer conditions over the BOB and Asian summer monsoon onset occurs.

## 1. Introduction

The Asian summer monsoon (ASM) onset is an important part of the seasonal transition from winter to summer. Many studies (Wu and Zhang 1998; Mao et al. 2002a; Wang and LinHo 2002; Mao and Wu 2007) have pointed out that the ASM onset starts over the eastern Bay of Bengal (BOB) area, followed by onset over the South China Sea (SCS) and finally by onset over India. Krishnamurti et al. (1981) identified a type of low-level vortex known as the onset vortex, which forms during the Indian summer monsoon onset at about 10°N in the BOB and eastern Arabian Sea (Ananthakrishnan et al. 1968). As the vortex moves northward and develops, the Indian summer monsoon is established (Vinayachandran et al. 2007). Features of the vortex, such as its structure

*Corresponding author address:* Dr. Guoxiong Wu, State Key Laboratory of Numerical Modeling for Atmospheric Sciences and Geophysical Fluid Dynamics (LASG), Institute of Atmospheric Physics, Chinese Academy of Sciences, P.O. Box 9804, Beijing 100029, China.
E-mail: gxwu@lasg.iap.ac.cn

DOI: 10.1175/JCLI-D-12-00286.1

and rainfall distribution, have been studied previously (Pisharoty and Asnani 1957; Rao and Rajamani 1970; Sharma and Srinivasan 1971). Atmospheric barotropic instability associated with horizontal wind shear, together with diabatic heating, is thought to be responsible for the vortex formation (Krishnamurti et al. 1981; Krishnamurti 1981, 1985; Krishnamurti and Ramanathan 1982; Mao and Wu 2011). Mak and Kao (1982) showed that vertical wind shear and baroclinic instability are also important for the vortex development. In addition to these internal dynamics, Joseph (1990) proposed that the vortex is also influenced by the local sea surface temperature (SST) because, if the SST is above 28°C and if other factors are favorable, organized deep convection will develop in the tropical atmosphere (Gray 1968, 1975, 1998; Harr and Chan 2005). Usually, a warm pool (SST $>$ 30.5°C) appears over the Arabian Sea about 1 week before the Indian summer monsoon onset. The warm SST leads to the formation of a vortex that affects the Indian summer monsoon onset over Kerala in early June (Joseph 1990; Shenoi et al. 1999, 2005).

The monsoon onset vortex (MOV) also exists over the BOB in early May during the BOB summer monsoon onset (Lau et al. 1998; He and Shi 2002; Liu et al. 2002; Yan 2005). Case studies show that, while the onset vortex is moving northward over the BOB region, the wintertime zonally oriented subtropical anticyclone belt splits over the BOB with the onset of the Asian summer monsoon (Mao et al. 2002b). Vinayachandran et al. (2007) studied the structure of the onset vortex and showed that the warmest SST is in the eastern BOB before the summer monsoon onset. Wu et al. (2011, 2012) emphasized the key role of air–sea interaction in the formation of the BOB MOV. They found that the strong surface sensible heating resulted from the BOB warm pool in spring leads to vortex formation. Previous research on the MOV has been confined to case studies. The current study will focus on climate-mean characteristics of the MOV formation and development in order to improve our understanding of the BOB summer monsoon onset process.

In addition to the lower-tropospheric circulation associated with the vortex, the upper-tropospheric circulation over the BOB also undergoes noticeable changes in the seasonal transition from winter to summer. Mao et al. (2004) pointed out that this seasonal transition starts with the occurrence of northward tilting of the subtropical ridge surface and a positive meridional temperature gradient (MTG) in the upper troposphere over the BOB. The ridgelines always tilt toward the warmer region with increasing height, and the moment when this tilt becomes perpendicular (i.e., $\partial T/\partial y = 0$) is defined as the monsoon onset time in the region. Based on such a concept, a series of the onset dates of the BOB summer monsoon has been produced (Mao and Wu 2007).

The SAH is another characteristic synoptic system over the Asian continent in boreal summer (Mason and Anderson 1958), which forms near the tropopause over the Indochinese peninsula before the BOB monsoon onset (He et al. 2006; Liu et al. 2009, 2012). The SAH is a thermal high pressure system, whose intensity depends on the distribution of heterogeneous diabatic heating over the Tibetan Plateau and the Asian summer monsoon area (Wu and Liu 2003; Wu et al. 2007). Its seasonal evolution and variation in boreal summer also depend strongly on changes in atmospheric heating, especially the thermal effect of the Tibetan Plateau (Flohn 1960; Krishnamurti and Rodgers 1970; Krishnamurti 1971a,b; Liu et al. 2001; Zhang et al. 2002; Wu et al. 2002; Qian et al. 2002; Duan and Wu 2005; Duan et al. 2008). Data diagnoses (Reiter and Gao 1982; Zhu et al. 1986; Chen et al. 1991) demonstrate that the SAH first appears in spring over the SCS just prior to the ASM onset. During the BOB monsoon onset, its center moves northwestward and intensifies over the Indochinese peninsula. Finally, after the ASM onset, it settles over the southern flank of the Tibetan Plateau.

It is still not clear how the SAH is generated in spring and how its development in the upper troposphere can help the MOV development, which has previously been thought to arise solely through air–sea interaction and energy conversions over the BOB, and contribute to the ASM onset. We address these questions in the current study. The remainder of this paper is organized as follows: Section 2 describes the data and method applied in this study. Section 3 investigates the variation in the SAH during the BOB summer monsoon onset, emphasizing the mechanism for the SAH formation and evolution. Section 4 describes the climate characteristics of the BOB MOV, focusing on the coupling between the upper and lower synoptic systems and summarizing the three-dimensional (3D) features of the BOB summer monsoon onset process. Finally, a discussion and summary are provided in section 5.

## 2. Data and methodology

The datasets used in this study are as follows: 1) The 40-yr European Centre for Medium-Range Weather Forecasts (ECMWF) Re-Analysis (ERA-40) (Uppala et al. 2005) data are for the period 1979–2001, including 3D wind field, geopotential height, air temperature, relative humidity, precipitation, and surface heating flux, with a horizontal resolution of 2.5° $\times$ 2.5°. The variables are arranged on standard isobaric surfaces from 1000 hPa

to 1 hPa, excluding the surface values. For consistency, the rainfall records within the ERA-40 dataset are directly applied in the present study. Except for excessive precipitation in the tropics, the ERA-40 rainfall data are shown to be reliable in comparison with other precipitation data derived from satellites, such as the 3B42 products of the Tropical Rainfall Measuring Mission (TRMM) and daily precipitation records of the Global Precipitation Climatology Project (GPCP) (Voisin et al. 2008; Chan and Nigam 2009). 2) Daily global sea surface winds with a high horizontal resolution of 0.25° × 0.25° are supplied by the National Oceanic and Atmospheric Administration (NOAA) (Zhang et al. 2006) and National Climatic Data Center (NCDC) (Smith and Reynolds 2004). In this dataset, the wind speeds are generated by blending observations from six satellites and the wind directions from the National Center for Environment Prediction/Department of Energy Global Reanalysis 2 (NCEP-2) dataset (Kanamitsu et al. 2002) are interpolated into the blended speed grids. 3) Daily optimum interpolation SST (OISST) analysis data (AVHRR products) are from the NOAA Satellite and Information Service with the same resolution as the sea surface winds. 4) Daily sea surface sensible heating flux with a horizontal resolution of 1° × 1° are obtained from objectively analyzed air–sea fluxes (OAFlux) for the global oceans, sponsored by the Woods Hole Oceanographic Institution (WHOI) Cooperative Institute for Climate and Ocean Research (CICOR).

In our composite study of the monsoon onset processes, it is important to have a robust definition of the onset date. As mentioned above, the earliest ASM onset is the BOB monsoon onset. In this study, we will focus on the BOB monsoon onset. Following Mao and Wu (2007), the BOB onset date is defined as the day when the following criteria are satisfied: 1) the area-averaged upper-tropospheric (200–500 hPa) MTG over the eastern BOB (5°–15°N, 90°–100°E) changes from negative to positive and 2) the MTG remains positive for more than 10 days. Table 1 lists the resultant BOB summer monsoon onset dates from 1979 to 2001. The mean onset date of the BOB summer monsoon is 2 May. The ECMWF Interim Re-Analysis (ERA-Interim) dataset (Dee et al. 2011) for the period 1979–2010 has been employed to verify what is shown in Table 1, and the results are quite similar. Other criteria for the monsoon onset are also used for comparison purpose, including the area-averaged 850-hPa zonal wind (U850) and outgoing longwave radiation (OLR) reaching threshold values of 0 m $s^{-1}$ and 230 W $m^{-2}$, respectively. The correlation coefficients of the MTG with U850 and with OLR are 0.94 and 0.67, respectively, with both above the 99% statistical significance level (0.481), indicating that the onset date defined by the sign change of MTG is reliable. The marked interannual variability of the BOB summer monsoon onset date requires us to use a composite analysis technique described below to obtain climate means of monsoon onset processes. For each individual year the onset date is defined as the zero day (D0), with the dates before (after) the onset date being labeled as negative (positive) days. All the variables are chosen from −30 days (D−30) to +30 days (D+30) relative to the BOB summer monsoon onset date each year. The climate states of a particular variable for each of the 61 days (D−30 to D+30) during the summer monsoon onset are thus calculated by arithmetically averaging the data over each corresponding day for the period 1979–2001.

TABLE 1. The BOB summer monsoon onset date for years from 1979 to 2001. The letters "E" and "L" mark the monsoon onset occurring after an El Niño and a La Niña event, respectively.

| Year | Date | Year | Date |
|---|---|---|---|
| 1979 | 9 May | 1991 | 22 Apr |
| 1980 | 11 May | 1992 (E) | 6 May |
| 1981 | 7 May | 1993 | 19 May |
| 1982 | 22 Apr | 1994 | 1 May |
| 1983 (E) | 13 May | 1995 (E) | 7 May |
| 1984 | 11 Apr | 1996 (L) | 27 Apr |
| 1985 (L) | 16 Apr | 1997 | 16 May |
| 1986 | 9 May | 1998 (E) | 13 May |
| 1987 | 3 May | 1999 (L) | 9 Apr |
| 1988 | 2 May | 2000 (L) | 25 Apr |
| 1989 | 30 Apr | 2001 (L) | 29 Apr |
| 1990 | 14 May | | |

## 3. Evolution of the SAH before the BOB summer monsoon onset

Figure 1 shows the evolution of the atmospheric circulation at 150 hPa during the BOB summer monsoon onset. On D−15 and earlier (Fig. 1a), South Asia is dominated by a large anticyclone with its ridge axis extending from the equatorial central Pacific to the north Indian Ocean. There is no closed SAH at this time. By D−12 (Fig. 1b), as northerly develops over the eastern SCS between 10° and 20°N, a closed anticyclone (viz., the SAH) appears in the upper troposphere over the western SCS and the southeastern Indochinese peninsula. The SAH strengthens and moves westward from the SCS to the Indochinese peninsula from D−9 to D−6 (Figs. 1c,d); meanwhile, the ridgeline remains around 10°N with little northward migration. The SAH center starts to shift to the north of 10°N from D−6 to D0, with the streamline field to its south exhibiting a "trumpet" shape and strong divergence

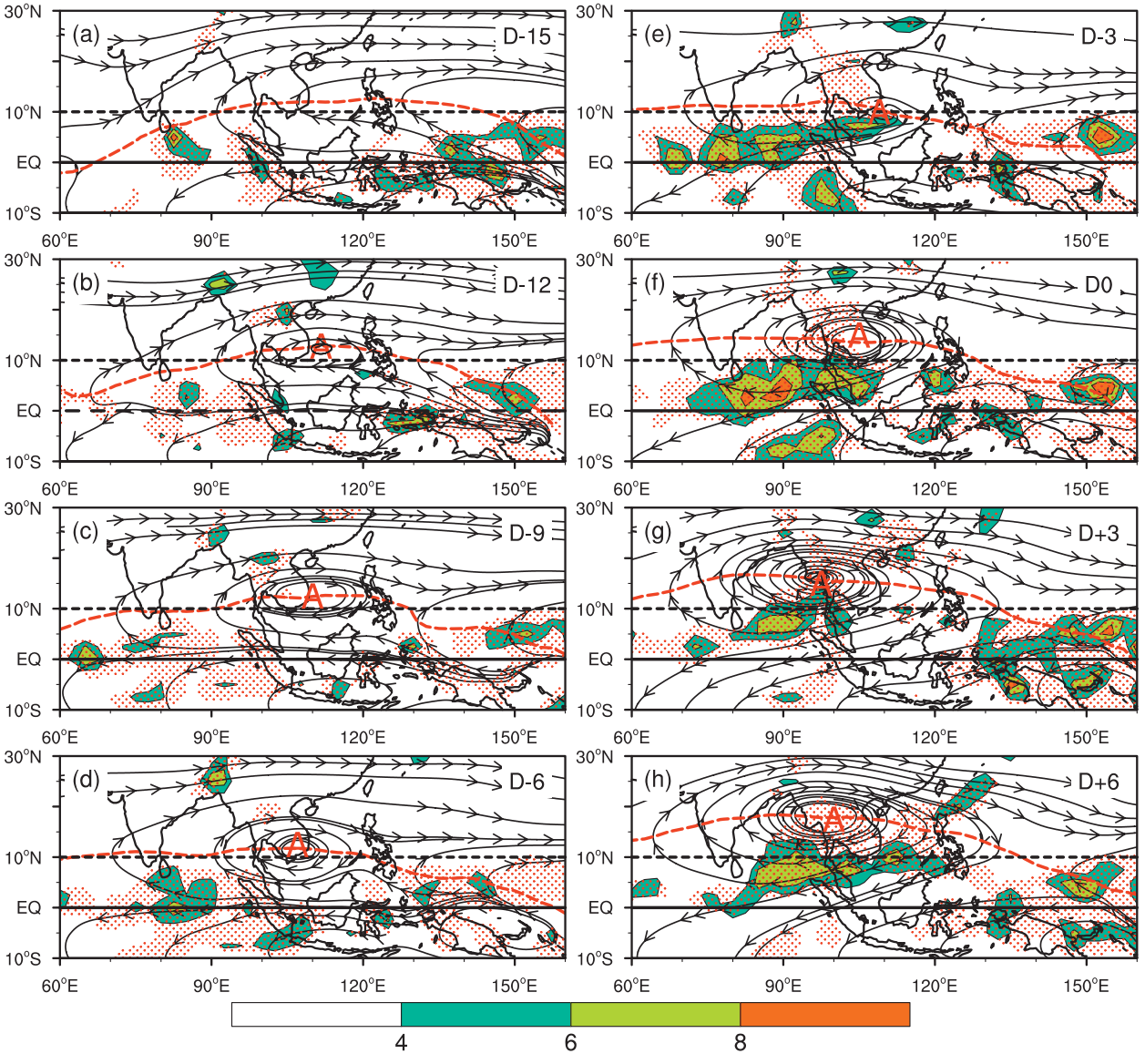


FIG. 1. Daily evolution of the 150-hPa streamline and divergent field (color shading, $10^{-6}$ s$^{-1}$) and the diabatic heating averaged from 500 to 200 hPa (red stippling, >1.5 K day$^{-1}$) during the BOB summer monsoon onset period: (a) D−15, (b) D−12, (c) D−9, (d) D−6, (e) D−3, (f) D0, (g) D+3, and (h) D+6. The letter "A" denotes the anticyclone center, and the ridgeline is plotted as a red dashed line.

over the southeastern BOB (Fig. 1e). When the BOB summer monsoon onset occurs on D0, the SAH shifts northward with its ridgeline situated near 15°N. The strong upper-level divergence persists over the southeastern BOB (Fig. 1f). After the summer monsoon builds up over the BOB, the SAH continues to develop and move farther northwestward (Fig. 1g). The center of the SAH is located near Yangon in Burma on D+6 (Fig. 1h), and the strong trumpet-shaped upper-layer divergence on its southwest persists and moves slowly eastward. The above results imply that the SAH evolution may be closely associated with the onset process of the BOB summer monsoon. We therefore consider below the SAH formation process prior to the BOB summer monsoon onset.

### *a. Formation of the SAH*

Figure 2 shows the geopotential height deviation from the zonal mean across South Asia in the premonsoon phase, averaged over 5°–15°N. On D−19 and D−16 in the upper troposphere, there is only one center above 150 hPa but two weak centers at 200 hPa, one over the SCS and the other over the ocean to the east of the Philippines (Figs. 2a,b). On D−13, the western high

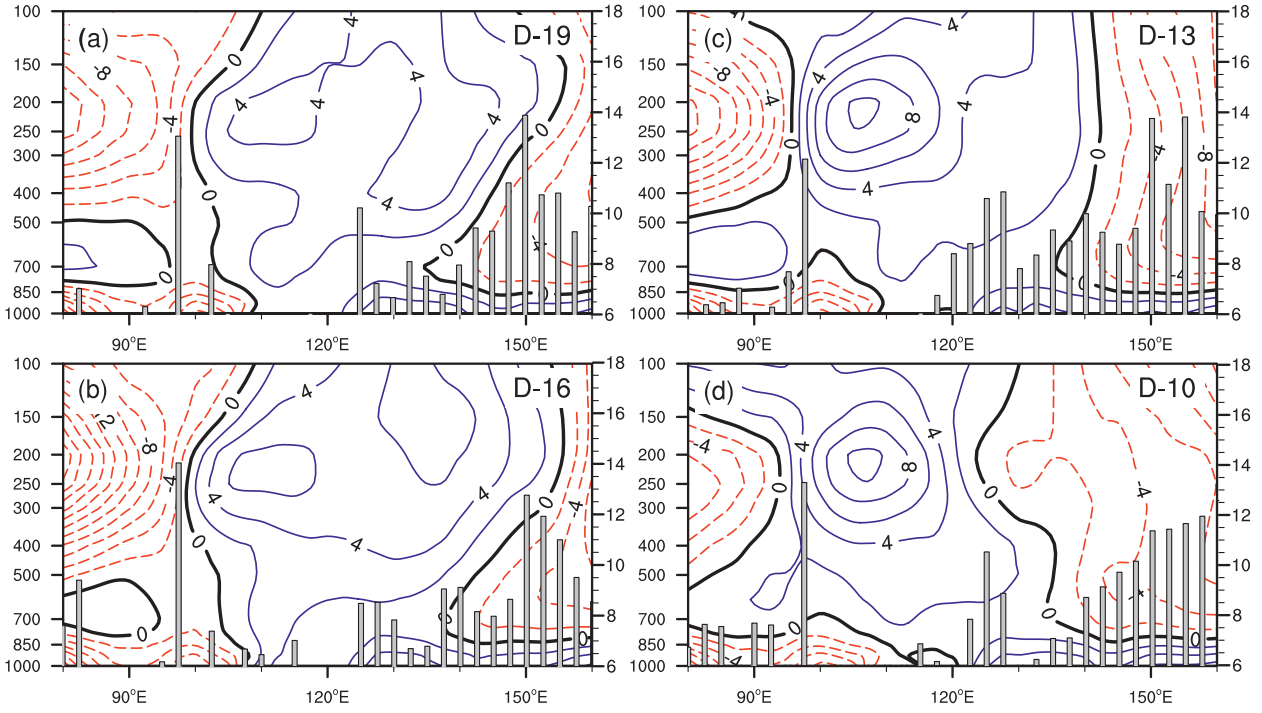


FIG. 2. Pressure–longitude cross section (averaged over 5°–15°N) of the deviation of geopotential height (contours, gpm) from the zonal mean: (a) D−19, (b) D−16, (c) D−13, and (d) D−10. The vertical bars represent the longitudinal profile of ERA-40 precipitation averaged over 5°–10°N (mm day$^{-1}$), with magnitude marked on the right vertical axis.

pressure center (i.e., the SAH) intensifies (Figs. 1b, 2c), while the eastern one weakens and disappears. Thus, the SAH formation presents as a substitution of the original anticyclone above the equatorial western Pacific by the western anticyclone over the western SCS and the southeastern Indochinese peninsula.

Note that, before the SAH formation phase from D−19 to D−16 (Figs. 2a,b), the main convection is over the western Pacific, with little rainfall over the SCS and the southeastern Indochinese peninsula (100°–120°E). On D−13 and D−10 (Figs. 2c,d), significant rainfall of more than 9 mm day$^{-1}$ occurs over the southern Philippines, but also little precipitation occurs over SCS. During this period, a northerly wind also develops in the upper troposphere over the eastern SCS (Figs. 1b,c), implying a potential association between the convection over the southern Philippines and the development of northerlies over the eastern SCS, which contributes to the generation of the SAH.

This relationship is investigated using the pressure–latitude cross section of local meridional circulation and diabatic heating averaged over the Philippines (120°–130°E) on D−19 and D−13 (Figs. 3a,b, respectively). Prior to SAH formation on D−19 (Fig. 3a), downward motion controls the southern Philippines region (around 10°N), with upper-layer southerlies above 500 hPa and lower-layer northerlies below. There is no apparent diabatic heating in the region. On D−13 (Fig. 3b), a strong deep convective condensation heating of more than 2.5 K day$^{-1}$ develops over the southern Philippines, and prevailing northerlies in the upper layers are established to the north of the heating region.

Following the Ertel potential vorticity equation (Ertel 1942; Hoskins et al. 1985), the vertical vorticity equation can be expressed as (Wu and Liu 1998; Wu et al. 1999; Liu et al. 1999, 2001, 2004)

$$\frac{\partial \zeta}{\partial t} + \mathbf{V}\cdot\nabla\zeta + \beta v = -(f+\zeta)\nabla\cdot\mathbf{V} + \frac{f+\zeta}{\theta_z}\frac{\partial Q}{\partial z} + S, \qquad (1)$$

in which the internal forcing term associated with atmospheric baroclinicity has been ignored because the current study focuses on the SAH that is in the upper troposphere in tropics, where the isentropic surfaces are horizontally located. On the right-hand side of Eq. (1), the three terms represent the effects of three-dimensional divergence and the vertical and horizontal gradients of diabatic heating, respectively. Scale analysis indicates that in the tropics the vorticity generation due to diabatic heating usually prevails over the atmospheric compressibility, and the first term on the right-hand side of Eq. (1) can be ignored as well. Within the heating

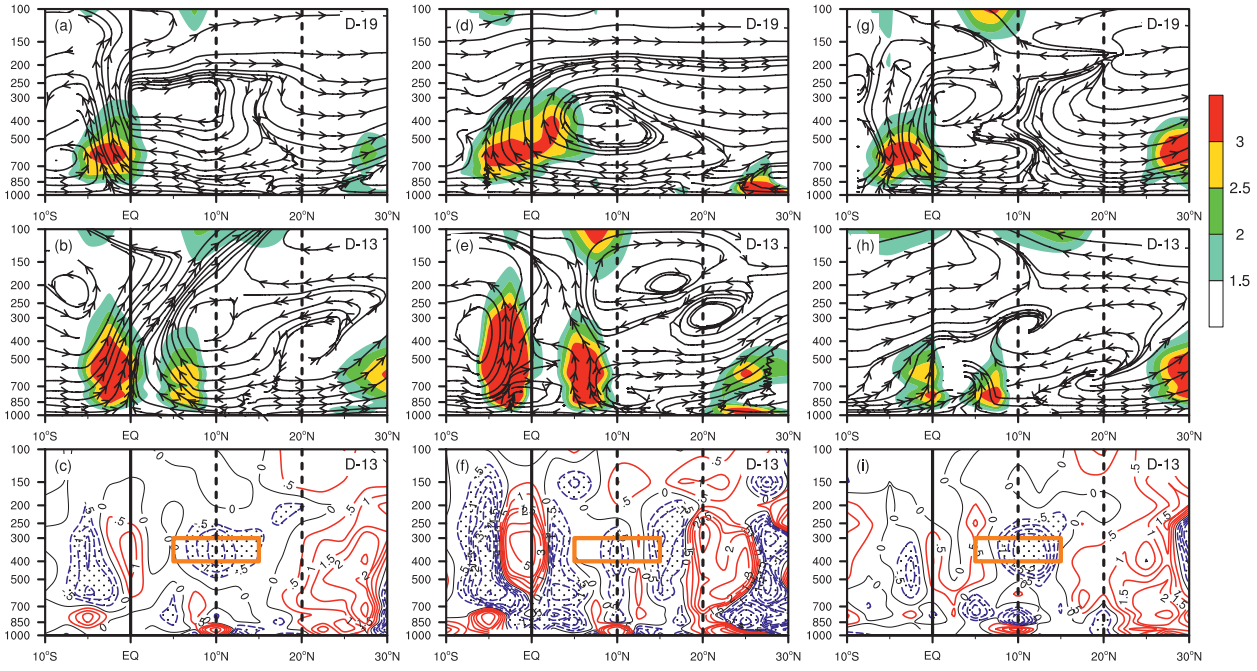


FIG. 3. The 120°–130° averaged pressure–latitude cross section of $Q_1$ (shaded, K day$^{-1}$) and meridional circulation on (a),(d),(g) D−19 and (b),(e),(h) D−13 and (c),(f),(i) of vorticity source $S$ on D−13 ($10^{-11}$ s$^{-2}$, values $> -0.5$ are stippled). Here, (a)–(c) are for the all-case composing, (d)–(f) are for the early group, and (g)–(i) are for the late group. The orange boxes in (c),(f),(i) denote the area with local maximum $S$.

region the vertical heating gradient ($\partial Q/\partial z$) dominates the forcing, whereas at the border of the diabatic heating the horizontal heating gradient (i.e., $S$) plays a more important role (Wu and Liu 1998; Liu et al. 2001). The vorticity source

$$S = -\frac{1}{\theta_z}\frac{\partial v}{\partial z}\frac{\partial Q}{\partial x} + \frac{1}{\theta_z}\frac{\partial u}{\partial z}\frac{\partial Q}{\partial y} = -\frac{g}{f\theta\theta_z}(\nabla_h\theta\cdot\nabla_h Q) \quad (2)$$

represents an external forcing caused by the correlation between the horizontal gradients of atmospheric temperature and diabatic heating. Here, $\theta_z$ and $Q$ are the static stability and diabatic heating source, respectively; $\mathbf{V}_h$ denotes horizontal gradient; and the other terms follow convention in meteorology. Of note is that $Q$ is calculated with the scheme deduced by Yanai et al. (1973), which takes the form

$$Q = Q_1 = C_p\left[\frac{\partial T}{\partial t} + \mathbf{V}\cdot\nabla_h T + \left(\frac{p}{p_0}\right)^{R/C_p}\omega\frac{\partial\theta}{\partial p}\right]. \quad (3)$$

Here $T$, $C_p$, and $R$ are the air temperature, the specific heat of dry air at constant pressure, and the gas constant for dry air, respectively. Atmospheric warming by latent heat release within tropical convection usually produces a warm core and an inward horizontal temperature gradient around the heating border. To the north of the heating, this gradient and the environmental MTG are positively correlated with the horizontal heating gradient. A negative vorticity source is then produced on the northern rim of the heating (Liu et al. 2001).

When convection develops over the southern Philippines on D−13, the strong local diabatic heating produces a considerable negative vorticity source ($< -2 \times 10^{-11}$ s$^{-2}$) in the upper troposphere to its north (Fig. 3c). The $S$ center over the Philippines is at 400–300 hPa. Accompanied by the occurrence of the negative vorticity source is a remarkable reversal of the upper-tropospheric circulation to its north: as shown in Figs. 3a and 3b in the latitude domain to the north of 10°N, the dominant southerly on D−19 is replaced by prevailing northerly on D−13. Because the northerly is produced in the upper troposphere along the longitude span between 120° and 130°E, which is located over the east of the SCS, the development of the northerly can help the isolation of an upper-layer anticyclone circulation over the SCS from the main anticyclone system over the western Pacific, in favor of the genesis of the SAH.

It should be noted that, in Table 1, the average onset date is 2 May, while the earliest onset date was 9 April in 1999 and the latest was 19 May in 1993; both are nearly 20 days away from the mean. The atmospheric state

during those extreme years can be closer to mid–late winter or midsummer, which may cause the composite results different substantially. To clarify the question, a standard deviation $\sigma$ of the monsoon onset day is calculated from the data listed in Table 1, and the thresholds of $\pm 0.7\sigma$ are chosen to select the early and late monsoon onset years. Five early years (1982, 1984, 1985, 1991, and 1999) and six late years (1980, 1983, 1990, 1993, 1997, and 1998) were then selected from the total 23 years, and three groups of onsets (all, early, and late) were composed. The evolutions for the early and late onset groups of diabatic heating, circulation, and relevant negative vorticity source $S$ near the Philippines are displayed in Fig. 3 in comparison with the composite (all case). As in the composite case, the diabatic heating centers in the early case (Figs. 3d,e) and the late case (Figs. 3g,h) both move northward to the southern Philippines from D−19 to D−13. In association with the northward displacement of the diabatic heating, a negative vorticity source ($S < 0$) appears in the mid–upper troposphere near 10°N in either the early case (Fig. 3f) or the late case (Fig. 3i). In each case in response to this negative vorticity forcing, the prevailing southerly in the upper troposphere over the latitude band 10°–20°N on D−19 (Figs. 3d,g) has been reversed to dominant northerly on D−13 (Figs. 3e,h) as in the all composite, which is in favor of the anticyclone vorticity formation over the SCS to its west. In view of the similar features of the different monsoon onset groups in the evolutions of diabatic heating, the occurrence of negative vorticity source near the southern Philippines, and the wind reversal over the eastern SCS, it is reasonably justified that the composite results presented in Figs. 3a–c are representative, even for both early and late monsoon onset groups.

Figure 4 presents the 400–300-hPa averaged horizontal distributions of $S$, $Q_1$, and streamline field on D−13 (Fig. 4a), also shown are the time series from D−19 to D+5 of $S$, $\mathbf{V}\cdot\nabla\zeta$, $\beta v$, and $(\mathbf{V}\cdot\nabla\zeta + \beta v)$ (Fig. 4b) averaged over the region (7.5°–12.5°N, 120°–125°E), an area of the south Philippines. It is evident that part of the negative vorticity source over the south Philippines is balanced by horizontal advection of relative vorticity due to the prevailing easterly across the source and by the horizontal advection of planetary vorticity due to the local northerly (Fig. 4a). Consequently, the streamline field exhibits a Gill-type response to the negative vorticity forcing source over the Philippines (Gill 1980), with the SAH establishing over the western SCS and the southeastern Indochinese peninsula. Afterward, although the stream field and the associated vorticity advection in the upper troposphere vary, the negative vorticity source over the Philippines remains stable at about $-1.0 \times 10^{-11}$ s$^{-2}$ until monsoon onset

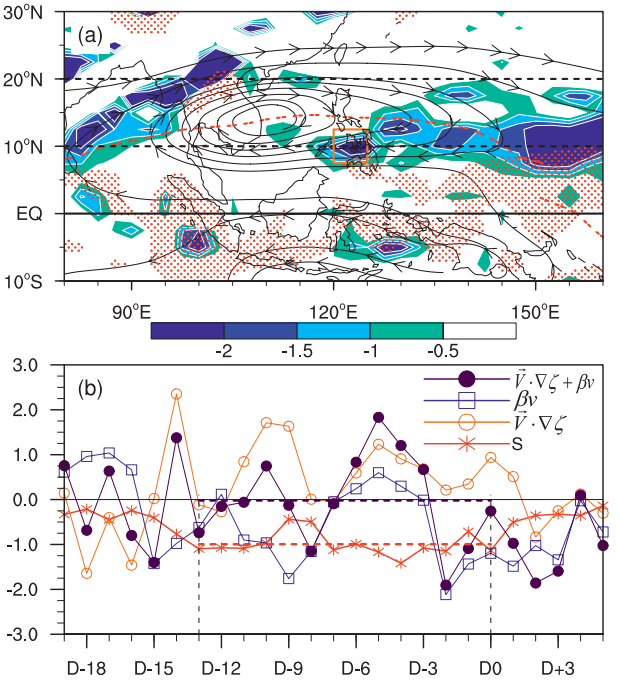


FIG. 4. (a) The 400–300-hPa averaged horizontal distributions of $S$ (shading, interval = $0.5 \times 10^{-11}$ s$^{-2}$), $Q_1$ (red stipple indicates > 1.5 K day$^{-1}$), and streamline field on D−13. (b) Time series of $S$, $\mathbf{V}\cdot\nabla\zeta$, $\beta v$, and $(\mathbf{V}\cdot\nabla\zeta + \beta v)$ over the region (7.5°–12.5°N, 120°–125°E) shown by the orange box in (a). The thick red (purple) dashed line in (b) represents the mean value of $S$ $(\mathbf{V}\cdot\nabla\zeta + \beta v)$ from D−13 to D0, respectively, and the vertical thin dashed lines in (b) are for the time point of D−13 and D0, respectively.

(Fig. 4b). The mean value of $S$ is one order of magnitude larger than the one of $(\mathbf{V}\cdot\nabla\zeta + \beta v)$ from D−13 to D0. Furthermore, the other forcing terms in (1) are small enough to be ignored. The stability and persistence of this near equatorial negative vorticity forcing source support the Gill-type atmospheric response to the negative vorticity forcing in the establishment of the SAH.

### b. *Strengthening of the SAH in the premonsoon period*

After D−13, the center of the SAH migrates gradually westward toward the Indochinese peninsula as its intensity increases (Fig. 1). Figure 5 shows the D−5 to D−1 averaged precipitation and circulation in the monsoon area. Over the northern Indochinese peninsula around 20°N, a rainfall center is isolated from the convection near the equator before the onset date (Fig. 5a). The condensation heating released by the rainfall center can produce negative relative vorticity and contribute to SAH strengthening in the upper troposphere.

During this period, there is strong surface sensible heating over the Indian peninsula, which contributes

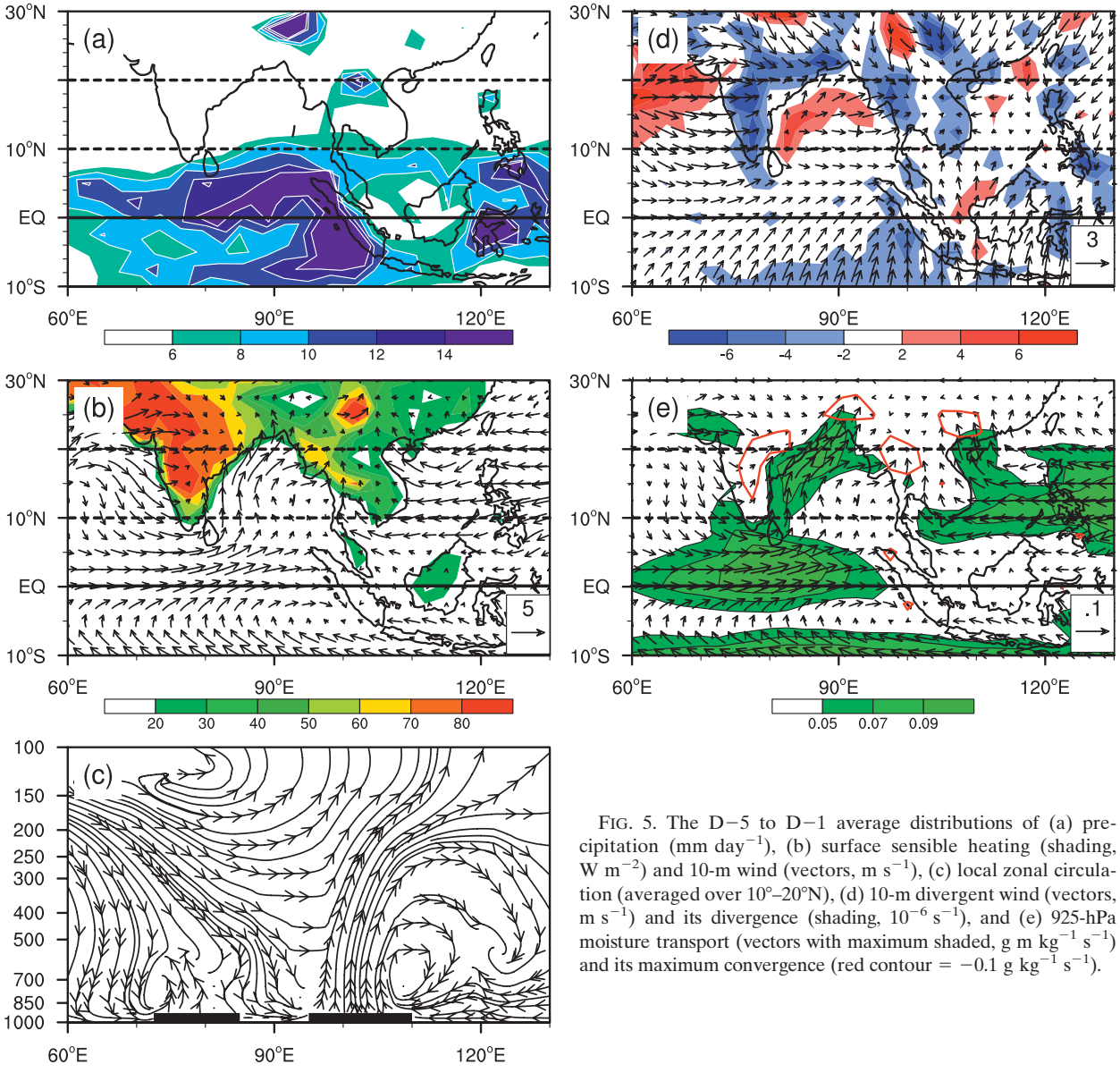


FIG. 5. The D−5 to D−1 average distributions of (a) precipitation (mm day$^{-1}$), (b) surface sensible heating (shading, W m$^{-2}$) and 10-m wind (vectors, m s$^{-1}$), (c) local zonal circulation (averaged over 10°–20°N), (d) 10-m divergent wind (vectors, m s$^{-1}$) and its divergence (shading, $10^{-6}$ s$^{-1}$), and (e) 925-hPa moisture transport (vectors with maximum shaded, g m kg$^{-1}$ s$^{-1}$) and its maximum convergence (red contour = −0.1 g kg$^{-1}$ s$^{-1}$).

substantially to the generation of a surface cyclone over land and anticyclones over the Arabian Sea and the northern BOB (Fig. 5b), accompanied by significant local descent (Fig. 5c). As the descending air reaches the sea surface, a divergent westerly develops with strong divergence over the ocean but convergence over the land (Fig. 5d). There are two water vapor paths surrounding the Indochinese peninsula: the southwesterly path over the northwestern BOB brings moisture to the Indochinese peninsula, while the southeasterly carries water vapor to the land from the SCS and west Pacific. The moisture moving from the ocean to the Indochinese peninsula is then transported northward by the strong lower-layer southerly (Fig. 5e). Moisture then converges near the northern Indochinese peninsula, contributing to the occurrence of the rainfall maximum there (Fig. 5a). Condensation heating due to the rainfall thus contributes to the development of the southerly in the lower layers and the strengthening of the SAH in the upper troposphere during the premonsoon period.

## 4. BOB summer monsoon onset process

As mentioned above, the SAH forms and develops before the BOB summer monsoon onset. Before we investigate the SAH impacts on the monsoon onset, we look at the onset processes. Based on case studies of the ASM onset in 1998 and 2003, Wu et al. (2011, 2012) have

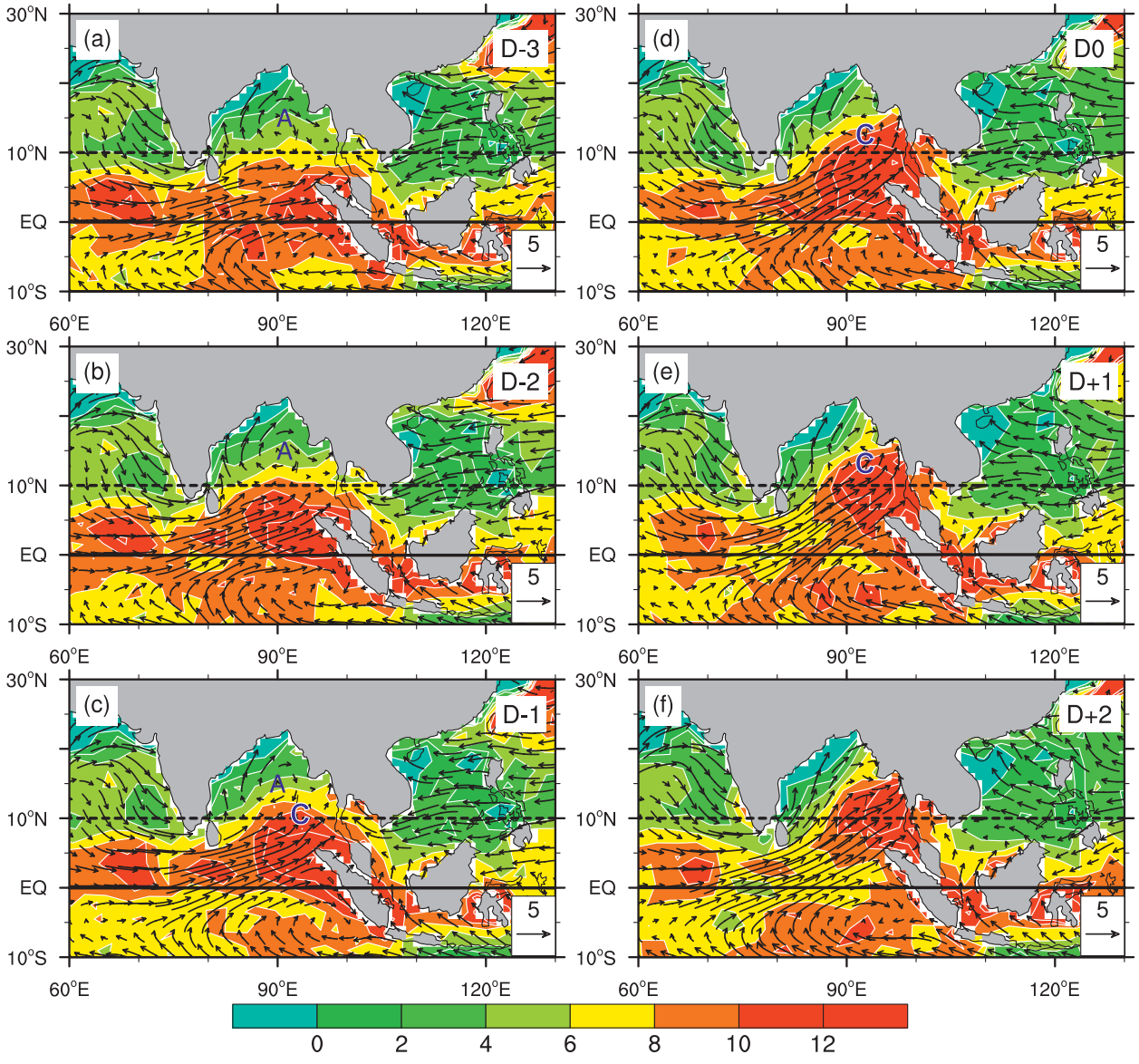


FIG. 6. Daily evolution of sea surface sensible heating (shading, W $m^{-2}$) and sea surface wind (vectors, m $s^{-1}$) for (a)–(f) D−3 to D+2. The letters "A" and "C" denote the anticyclone and cyclone centers, respectively.

reported that air–sea interaction plays an important role in the MOV formation during the BOB summer monsoon onset. In this section, the composite technique is employed again to study the climate-mean characteristics of the MOV formation and its connection with the ASM onset.

### *a. Generation of the MOV*

Both the atmospheric circulation and the thermal conditions on the sea surface change distinctly during the BOB summer monsoon onset. Before the onset, strong sensible heating (>12 W $m^{-2}$) is observed beneath the strong equatorial surface westerly over the southern BOB (Figs. 6a–c). At 700 hPa, a distinct local cyclonic circulation pattern over the tropical BOB develops in response to this sensible heating (Figs. 7a–c). The SST in the southeastern BOB is relatively colder than the one in the central BOB (Fig. 9). One possible reason is that, over the southern BOB, the stronger surface westerly prevents the local SST from rapidly rising up through the wind–evaporation–SST feedback (Xie and Philander 1994). Furthermore, the near-equatorial cloud related to local rainfall could also inhibit the solar radiation from warming the SST directly. Over the northern BOB,

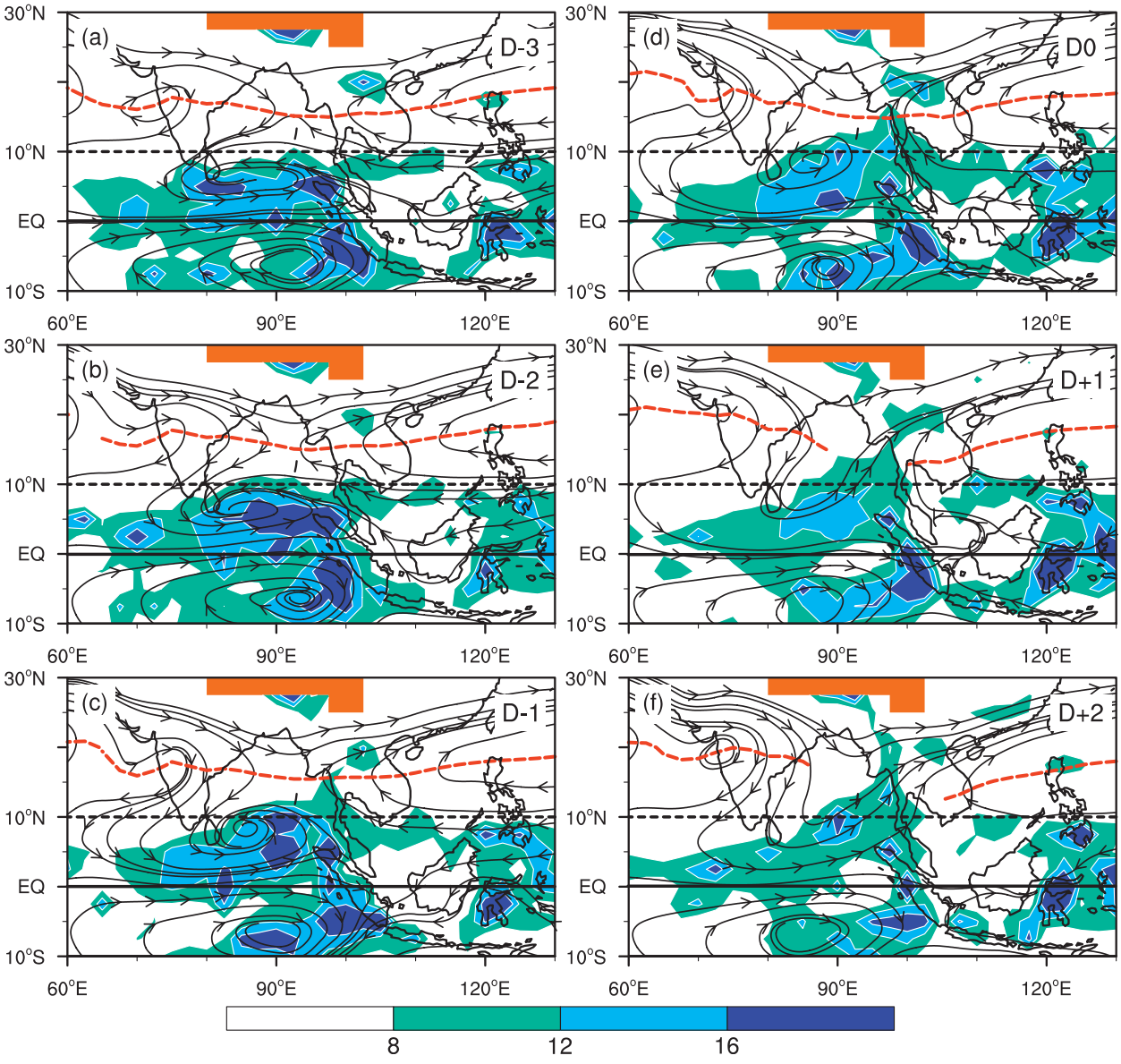


FIG. 7. Daily evolution of 700-hPa streamlines and ERA-40 rainfall (shading, mm day$^{-1}$) for (a)–(f) D−3 to D+2. Topography and ridgeline are marked by orange area and red dashed line, respectively.

a distinct anticyclone is situated near the surface (Figs. 6a–c) and a continuous ridgeline of the subtropical anticyclone is located at 700 hPa with a weak Indo-Burma trough over the eastern BOB (Figs. 7a–c). These features are associated with downward motion (Fig. 5c) with diabatic cooling (Figs. 8a–c) over the northern BOB. The resultant clear sky and weak surface wind conditions favor increasing solar radiation and decreasing energy release from the ocean, as reported by Wu et al. (2011, 2012), and a warm pool (SST > 30°C) is formed between 10° and 15°N over the central BOB before the summer monsoon onset (Figs. 9a–c). This short-lived warm pool in spring only occurs over the central eastern BOB, because before the BOB summer monsoon onset the prevailing southwesterly winds along the northwestern BOB (Figs. 6a–c) cause upwelling in the region due to the offshore currents and a buildup of cold sea surface water (Figs. 9a–c). A similar situation exists over the northeastern BOB because of the prevailing surface northerly winds.

After the summer monsoon onset, the southwesterly sweeps over most of the central and eastern BOB and induces onshore currents along the eastern coast (Figs. 6d–f), with local downwelling maintaining warm SST

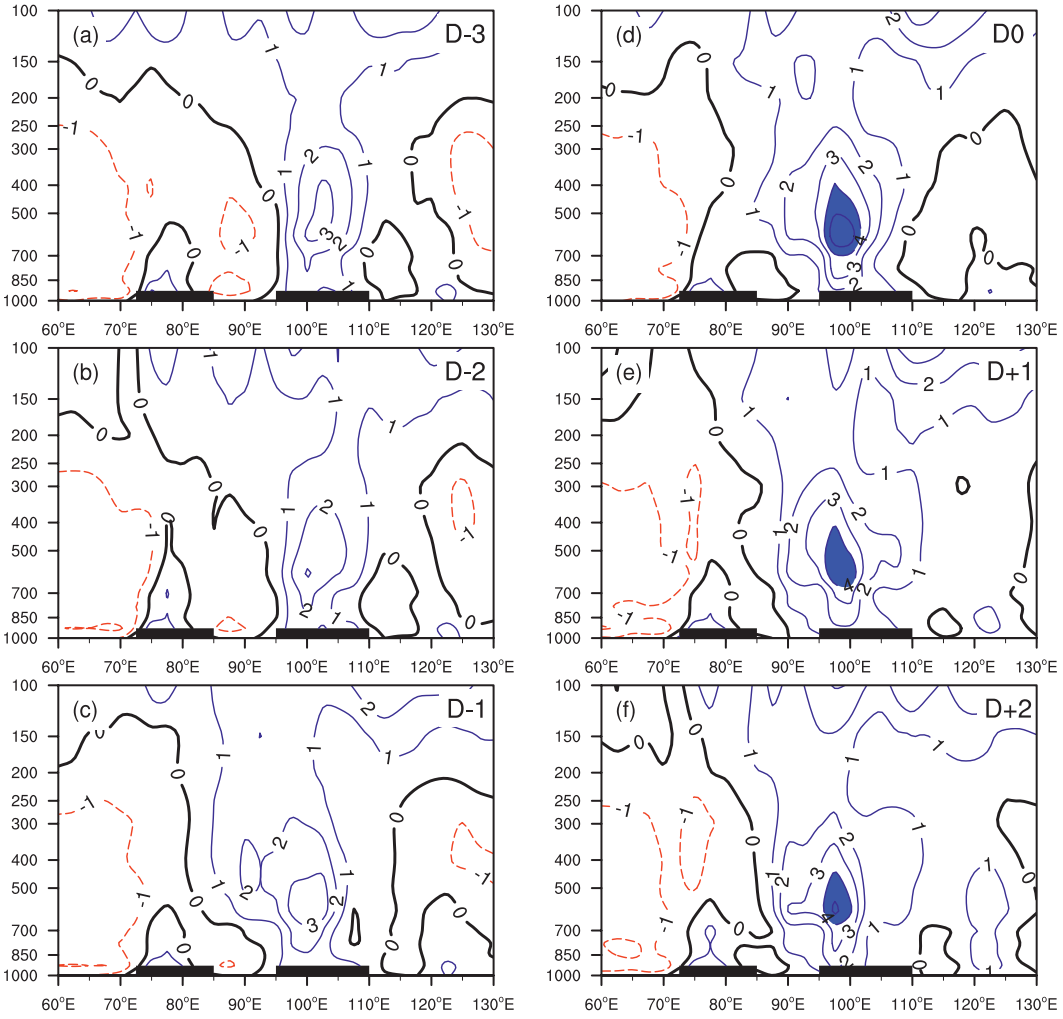


FIG. 8. Daily evolution of the 10°–20°N averaged pressure–longitude cross section of apparent heating source $Q_1$ (K day$^{-1}$, values $>$ 4 K day$^{-1}$ shaded) for (a)–(f) D−3 to D+2.

there. This, together with the increased local surface wind, enhances the local surface sensible heating. As the atmosphere is heated in an already warm area over the ocean warm pool, atmospheric available potential energy is generated; cyclonic circulation or even a MOV develops in the region. The positive feedback due to local air–sea interaction supports further development and northward displacement of the MOV even after the onset date (Fig. 6e).

At 700 hPa, the cyclone near Sri Lanka also moves northward (Fig. 7d). As the MOV develops, the cyclone merges with the Indo-Burma trough and the subtropical high ridgeline splits. Consequently, the equatorial westerly over the southern BOB is linked directly with the subtropical westerly over the central Indochinese peninsula and the southern coast of China, and abundant water vapor is transported to the Indochinese peninsula, accompanied by heavy rain over the northeastern BOB and the western Indochinese peninsula (Figs. 7e,f, 8d–f). The ASM onset commences.

### b. *Evolution of the SAH*

During the BOB summer monsoon onset the SAH also develops significantly, as shown in Fig. 1 (right). On D−3 the anticyclone center is still over the southeast of the Indochinese peninsula with its ridgeline at 10°N over the BOB (Fig. 1e), and the divergence on its southwest over the southern BOB is weak. From D−3 to D0 (Fig. 1f), the ridgeline shifts rapidly from 10° to 15°N, and the upper divergence to the southwest of the SAH center strengthens significantly, reaching a maximum value of more than $8 \times 10^{-6}$ s$^{-1}$ over the southern BOB. After the ASM onset (Figs. 1g,h), the SAH strengthens and its center moves farther northward, and the

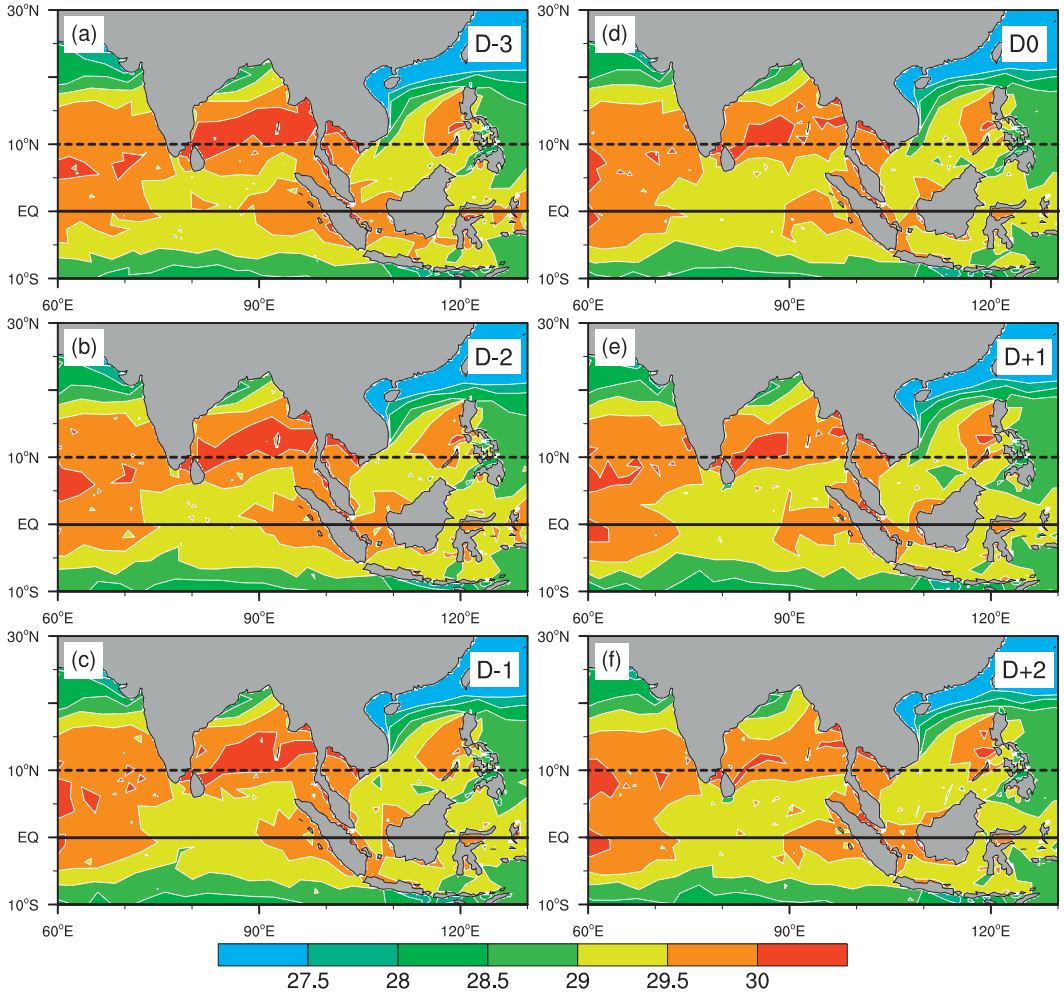


FIG. 9. Daily evolution of sea surface temperature (°C) for (a)–(f) D−3 to D+2.

trumpet-shaped strong upper-layer divergence on its southwest persists and moves slowly eastward.

This evolution of the SAH in the upper troposphere strongly influences the MOV generation near the surface and the ASM onset. Figure 10 shows the 3D structure of the atmospheric circulation during the MOV formation process. On D−3 (Fig. 10a), a belt of weak positive surface relative vorticity lies over the southern BOB, with a band of surface wind cyclonic shear just to the south of the surface anticyclone over the northern BOB. Meanwhile, the SAH ridgeline is located near 10°N, with persistent upper-tropospheric divergence of more than $4 \times 10^{-6}$ s$^{-1}$ to its south. While the SAH is moving northward from D−3 to D0 (Figs. 1e,f), the upper-layer divergence becomes more organized and stronger ($>8 \times 10^{-6}$ s$^{-1}$) over the southern BOB (Fig. 10b). The strong ascending motion at 600 hPa is better correlated with the maximum of upper-layer divergence than with the large value of the lower cyclonic vorticity over the southern BOB. This implies a close coupling between the upper-layer divergence and midlayer air ascent: that is, a pronounced pumping effect above the southern part of the BOB during the gestation of the MOV. On D−1 (Fig. 10c), the very strong upper-layer divergence, the midtroposphere ascent, and the strong surface vorticity are all well coupled: they become perpendicular near 10°N where the MOV appears (Fig. 6c). As mentioned above, the SST in the southeastern BOB is relatively colder compared to the central BOB (Fig. 9); therefore, this strong pumping effect can be considered as a trigger for the formation of the MOV. After the BOB summer monsoon onset, the SAH ridgeline remains near 15°N over the northern BOB (Figs. 10e,f). The MOV continues to move northeastward into the warm pool area over the northeastern BOB where surface winds intensify and sea surface sensible heating strengthens rapidly (Figs. 6d–f). The positive feedback due to air–sea interaction further promotes

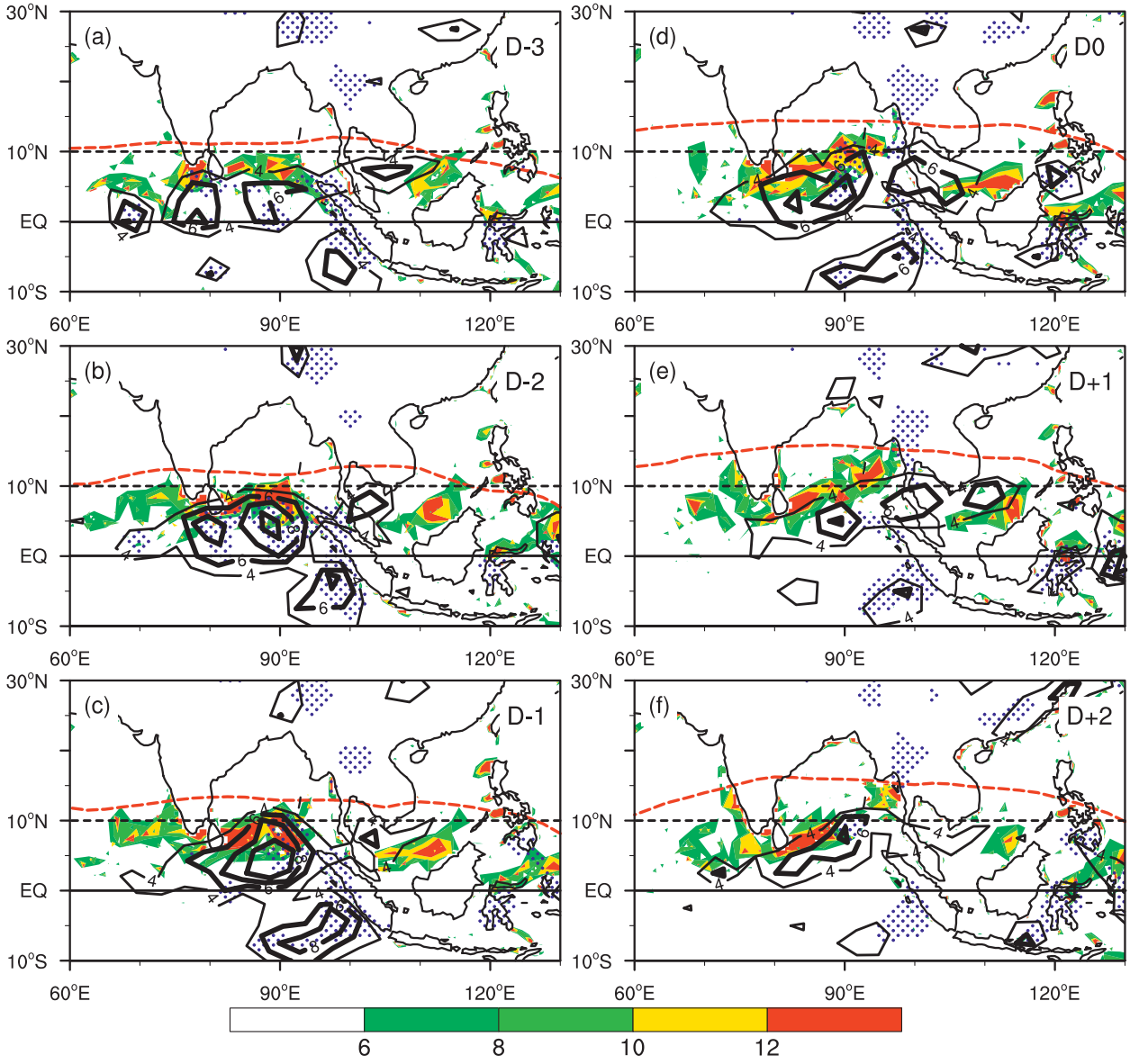


FIG. 10. Daily evolution of 150-hPa divergence (black solid contours, interval = $2 \times 10^{-6}$ s$^{-1}$; thicker line values > 6) and ridgeline of the SAH (red dashed line), 600-hPa ascending motion (blue stippled area, only values < −0.08 Pa s$^{-1}$ are plotted), and sea surface positive relative vorticity (shading, $10^{-6}$ s$^{-1}$) for (a)–(f) D−3 to D+2.

development of the MOV after the BOB summer monsoon onset. Moreover, the positive meridional gradient of SST over the BOB could facilitate northward advance of the MOV. Deep convection then commences over the northeastern BOB and Indochinese peninsula as the MOV merges into the Indo-Burma trough, accompanied by the splitting of the subtropical anticyclone ridgeline (Figs. 7e,f). The strong condensation heating released by the deep monsoon convection sustains the SAH over the peninsula (Figs. 1g,h). However, although the upper-layer divergence is still maintained over the southern BOB, it is decoupled from the atmospheric ascent in the middle layer and the vortex near the surface (Figs. 10e,f). Consequently, the surface vortex ceases to develop and finally disappears on D+2 (Fig. 6f).

## 5. Summary and discussion

Composite analysis based on the ERA-40 dataset has been used to study the climate-mean characteristics of the generation of the SAH, the Asian summer monsoon

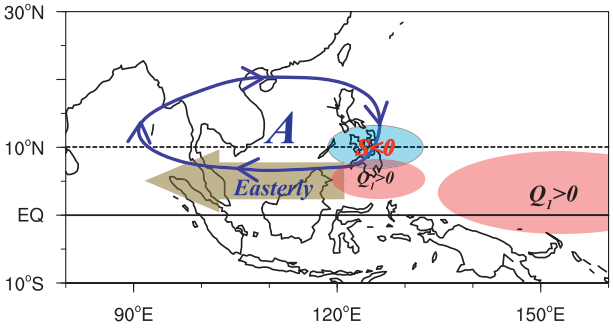


FIG. 11. Schematic diagram presenting the mechanism responsible for the SAH (marked by *A*) formation: persistent convective diabatic heating in spring over the south Philippines produces a sustained negative vorticity source over the Philippines, and the South Asian high is generated as a Gill-type atmospheric response to the negative forcing source. The marked area over the equatorial west Pacific denotes the diabatic heating, which is isolated from the one over the south Philippines.

onset process, and the impacts of the SAH on the BOB MOV formation and monsoon onset. In the East Asian and western Pacific areas as the season evolves from winter to spring, the center of the lower-tropospheric anticyclone shifts gradually from eastern China to the western Pacific. By April and early May, the moist tropical southeasterly that originates from the western Pacific ''warm pool'' region merges into the subtropical easterly on the south of the anticyclone, then hits the warm land of the south Philippines and triggers local convective instability. Convection and the related diabatic heating strengthen noticeably over the southern Philippines about a fortnight before the ASM onset and persist in the region until the ASM onset. A persistent negative vorticity source ($S < 0$) in the mid–upper troposphere is induced poleward of the convection center as illustrated schematically in Fig. 11. The SAH is thus generated to the northwest of the persistent negative vorticity source $S$ and the resultant streamline field manifests itself as a Gill-type response (Gill 1980). Meanwhile, an abnormal cyclone develops in the upper troposphere over the equatorial western Pacific, causing the original anticyclone to weaken and eventually disappear. Thus, both the development of an anticyclone over the western SCS and southeastern Indochinese peninsula and the dampening of the original anticyclone over the equatorial west Pacific contribute to the SAH formation.

In the lower troposphere, strong sensible heating over the Indian peninsula produces a surface anticyclone and downward flow over the northern BOB prior to the BOB monsoon onset. Strong divergent wind from the surface anticyclone brings abundant moisture into the Indochinese peninsula. The surface southerlies then transport the vapor to the north where heavy rainfall develops. The latent heat release associated with precipitation then contributes to the westward movement and intensification of the SAH after it is generated.

The development of the surface anticyclone over the northern BOB in spring provides favorable conditions for the formation of a short-lived warm pool over the central BOB and contributes to the genesis of the MOV over the BOB just before the monsoon onset. In the upper troposphere, owing to the development of the SAH, the upper-layer divergence on the southwestern side of the SAH increases over the southern BOB and is then coupled with stronger ascending motion in the middle troposphere. Such a pumping effect triggers the genesis of the MOV near the surface and intensifies the surface southwesterly over the northeastern BOB. Subsequently, the development of onshore ocean currents and downwelling near the coast maintains the local warm SST and the surface sensible heating is enhanced over the eastern BOB. As a consequence, the MOV develops further during and even after the monsoon onset. At 700 hPa, in tandem with the northeastward development of the surface MOV, the tropical cyclone moves northward and merges into the Indo-Burma trough and the original zonally oriented subtropical high over the northern BOB splits. Thus, the southwesterly in front of the trough brings abundant moisture to the Indochinese peninsula, where deep convection builds up. Torrential rainfall develops over the eastern BOB and western Indochinese peninsula, and the ASM onset thus commences over the eastern BOB. In short, the ASM onset occurs firstly over the eastern BOB because of a close coupling between the upper-tropospheric pumping because of the development of the SAH and the near surface air–sea interaction on the BOB. The pumping effect due to the strengthening of the SAH triggers the MOV genesis, and the local air–sea interaction plays a key role in the MOV development, which contributes to the BOB summer monsoon onset.

Our results, which are based on a climate-mean analysis, demonstrate the impact of coupling between air–sea interaction and SAH evolution on the BOB MOV formation and development. However, the MOV formation process can be very different from year to year because of the pronounced interannual variability of the BOB summer monsoon onset. In the ocean, the warm pool formation is affected by both the solar radiation and the mixed-layer depth; the earlier (later) the summer monsoon onset, the shorter (longer) the warming time of SST by solar radiation before the monsoon onset and so the colder (warmer) the SST. It is also true that the shallower the mixed-layer depth, the easier it is for a warm pool to form. Thus, the influence of air–sea

interaction is different from year to year. In the atmosphere, the major factors that affect the SAH generation and evolution, including the condensation heating over the southern Philippines and the moisture transport and the sensible heating over the Indochinese peninsula, also possess distinct individual variability. In addition, as shown in Table 1 there is close relationship between the onset time of BOB summer monsoon and ENSO events: that is, early onset after the La Niña events but late onset after the El Niño events. The work of Wu and Zhang (1998) has also demonstrated that the ASM onset is strongly modulated by the intraseasonal oscillations from the south, east, and northwest directions. How the ENSO events and ISOs affect the interannual variation of the Asian monsoon onset is still unclear. Therefore, further studies on the interannual variability of the coupling between the SAH evolution and air–sea interaction are required for a comprehensive understanding of the dynamical processes of the Asian summer monsoon onset.

*Acknowledgments.* The authors thank the three anonymous reviewers for their constructive suggestions. This study was jointly supported by the MOST Program 2010CB950400 and 2012CB417200 and the NSFC Projects 40875034, 40925015, 41175059, and 41275088.

## REFERENCES

Ananthakrishnan, R., V. Srinivasan, A. Ramakrishnan, and R. Jambunathan, 1968: Synoptic features associated with onset of southwest monsoon over Kerala. India Meteorological Department Forecasting Manual IV-18.2, 17 pp.

Chan, S. C., and S. Nigam, 2009: Residual diagnosis of diabatic heating from ERA-40 and NCEP reanalyses: Intercomparisons with TRMM. *J. Climate,* **22,** 414–428.

Chen, L. X., Q. Zhu, H. Luo, J. He, M. Dong, and Z. Feng, 1991: *East Monsoon* (in Chinese). China Meteorological Press, 362 pp.

Dee, D. P., and Coauthors, 2011: The ERA-Interim reanalysis: Configuration and performance of the data assimilation system. *Quart. J. Roy. Meteor. Soc.,* **137,** 553–597.

Duan, A. M., and G. Wu, 2005: Role of the Tibetan Plateau thermal forcing in the summer climate patterns over subtropical Asia. *Climate Dyn.,* **24,** 793–807.

——, ——, and X. Liang, 2008: Influence of the Tibetan Plateau on the summer climate patterns over East Asia in the IAP/LASG SAMIL model. *Adv. Atmos. Sci.,* **25,** 518–528.

Ertel, H., 1942: Ein neuer hydrodynamische wirbdsatz. *Metror. Z. Braunschweig.,* **59,** 33–49.

Flohn, H., 1960: Recent investigation on the mechanism of the 'summer monsoon' of southern and eastern Asia. *Proc. Symp. Monsoon of the World,* New Delhi, India, Hind Union Press, 75–88.

Gill, A. E., 1980: Some simple solutions for heat-induced tropical circulation. *Quart. J. Roy. Meteor. Soc.,* **106,** 447–462.

Gray, W. M., 1968: Global view of the origin of tropical disturbances and storms. *Mon. Wea. Rev.,* **96,** 669–700.

——, 1975: Tropical cyclone genesis. University of Colorado Atmospheric Science Paper 324, 121 pp.

——, 1998: The formation of tropical cyclones. *Meteor. Atmos. Phys.,* **67,** 37–39.

Harr, P. A., and J. Chan, 2005: Monsoon impacts on tropical cyclone variability. *The Global Monsoon System: Research and Forecast*, C.-P. Chang, B. Wang, and N.-C. G. Lau, Eds., Secretariat of the World Meteorological Organization, 512–542.

He, J. H., and X. Shi, 2002: Splitting and eastward withdrawal of the subtropical high belt during the onset of the South China Sea summer monsoon and their possible mechanism (in Chinese). *J. Nanjing Univ.,* **38,** 318–330.

——, M. Wen, L. Wang, and H. Xu, 2006: Characteristics of the onset of the Asian summer monsoon and the importance of Asian–Australian ''land bridge.'' *Adv. Atmos. Sci.,* **23,** 951–963.

Hoskins, B. J., M. Mclntyre, and A. Robertson, 1985: On the use and significance of isentropic potential vorticity maps. *Quart. J. Roy. Meteor. Soc.,* **111,** 877–946.

Joseph, P. V., 1990: Warm pool over the Indian Ocean and monsoon onset. *Trop. Ocean Atmos. Newsl.,* **53,** 1–5.

Kanamitsu, M., W. Ebisuzaki, J. Woollen, S. Yang, J. Hnilo, M. Fiorino, and G. Potter, 2002: NCEP–DOE AMIP-II Reanalysis (R-2). *Bull. Amer. Meteor. Soc.,* **83,** 1631–1643.

Krishnamurti, T. N., 1971a: Obserational study of the tropical upper troposhpheric motion field during the Northern Hemisphere summer. *J. Appl. Meteor.,* **10,** 1066–1096.

——, 1971b: Tropical east–west circulation during the northern summer. *J. Atmos. Sci.,* **28,** 1342–1347.

——, 1981: Cooling of the Arabian Sea and the onset-vortex during 1979. Recent progress in the equatorial oceanography. SCOR Working Group 47 Final Rep., 1–12. [Available from Nova University, Ocean Science Center, Dania, FL 33004.]

——, 1985: Summer monsoon experiment—A review. *Mon. Wea. Rev.,* **113,** 1590–1626.

——, and E. Rodgers, 1970: 200-mb wind field June, July, August 1967. Florida State University Department of Meteorology Rep. 70-2, 115 pp.

——, and Y. Ramanathan, 1982: Sensitivity of the monsoon onset to differential heating. *J. Atmos. Sci.,* **39,** 1290–1306.

——, P. Ardanuy, Y. Ramanathan, and R. Pasch, 1981: On the onset vortex of the summer monsoon. *Mon. Wea. Rev.,* **109,** 344–363.

Lau, K. M., H. Wu, and S. Yang, 1998: Hydrologic processes associated with the first transition of the Asian summer monsoon: A pilot satellite study. *Bull. Amer. Meteor. Soc.,* **79,** 1871–1882.

Liu, B. Q., J. He, and L. Wang, 2009: Characteristics of the South Asia high establishment processes above the Indochina peninsula from April to May and their possible mechanism (in Chinese). *Chin. J. Atmos. Sci.,* **33,** 1319–1332.

——, ——, and ——, 2012: On a possible mechanism for southern Asian convection influencing the South Asian high establishment during winter to summer transition. *J. Trop. Meteor.,* **18,** 473–484.

Liu, Y. M., G. Wu, H. Liu, and P. Liu, 1999: The effect of spatially nonuniform heating on the formation and variation of subtropical high. Part III: Condensation heating and South Asian high and western Pacific subtropical high (in Chinese). *Acta Meteor. Sin.,* **57,** 525–538.

——, ——, ——, and ——, 2001: Condensation heating of the Asian summer monsoon and the subtropical anticyclones in the eastern hemisphere. *Climate Dyn.,* **17,** 327–338.

——, J. Chan, J. Mao, and G. Wu, 2002: The role of Bay of Bengal convection in the onset of the 1998 South China Sea summer monsoon. *Mon. Wea. Rev.,* **130,** 2731–2744.

——, G. Wu, and R. Ren, 2004: Relationship between the subtropical anticyclone and diabatic heating. *J. Climate,* **17,** 682–698.

Mak, M., and C.-Y. J. Kao, 1982: An instability study of the onset-vortex of the southwest monsoon, 1979. *Tellus,* **34,** 358–368.

Mao, J. Y., and G. Wu, 2007: Interannual variability in the onset of summer monsoon over the eastern Bay of Bengal. *Theor. Appl. Climatol.,* **89,** 155–170.

——, and ——, 2011: Barotropic process contributing to the formation and growth of tropical cyclone Nargis. *Adv. Atmos. Sci.,* **28,** 483–491.

——, ——, and Y. Liu, 2002a: Study on modal variation of subtropical high and its mechanism during seasonal transition. Part I: Chimatological features of subtropical high structure (in Chinese). *Acta Meteor. Sin.,* **60,** 400–408.

——, ——, and ——, 2002b: Study on modal variation of subtropical high and its mechanism during seasonal transition. Part II: Seasonal transition index over Asian monsoon region (in Chinese). *Acta Meteor. Sin.,* **60,** 409–420.

——, J. Chan, and G. Wu, 2004: Relationship between the onset of the South China Sea summer monsoon and the structure of the Asian subtropical anticyclone. *J. Meteor. Soc. Japan,* **82,** 845–859.

Mason, R. B., and C. Anderson, 1958: The development and decay of the 100mb summertime anticyclone over southern Asia. *Mon. Wea. Rev.,* **91,** 3–12.

Pisharoty, P. R., and G. Asnani, 1957: Rainfall around monsoon depressions over India. *Indian J. Meteor. Geophys.,* **8,** 1–6.

Qian, Y. F., Q. Zhang, Y. Yao, and X. Zhang, 2002: Seasonal variation and heat preference of the South Asian high. *Adv. Atmos. Sci.,* **19,** 821–836.

Rao, K. V., and S. Rajamani, 1970: Diagnostic study of a monsoon depression by geostrophic baroclinic model. *Indian J. Meteor. Geophys.,* **21,** 187–194.

Reiter, E. R., and D. Gao, 1982: Heating of the Tibet Plateau and movements of the South Asian high during spring. *Mon. Wea. Rev.,* **110,** 1694–1711.

Sharma, M. C., and V. Srinivasan, 1971: Centres of monsoon depressions as seen in satellite pictures. *Indian J. Meteor. Geophys.,* **22,** 357–358.

Shenoi, S. S. C., D. Shankar, and S. Shetye, 1999: On the sea surface temperature high in the Lakshadweep Sea before the onset of the southwest monsoon. *J. Geophys. Res.,* **104,** 15 703–15 712.

——, ——, V. Gopalakrishna, and F. Durand, 2005: Role of ocean in the genesis and annihilation of the core of the warm pool in the southeastern Arabian Sea. *Mausam,* **56,** 147–160.

Smith, T. M., and R. Reynolds, 2004: Inproved extended reconstruction of SST (1854–1997). *J. Climate,* **17,** 2466–2477.

Uppala, S. M., and Coauthors, 2005: The ERA-40 Re-Analysis. *Quart. J. Roy. Meteor. Soc.,* **131,** 2961–3012.

Vinayachandran, P. N., D. Shankar, J. Kuria, F. Durand, and S. Shenoi, 2007: Arabian Sea mini warm pool and monsoon onset vortex. *Curr. Sci.,* **93,** 203–214.

Voisin, N., A. Wood, and D. Lettenmaier, 2008: Evaluation of precipitation products for global hydrological prediction. *J. Hydrometeor.,* **9,** 388–407.

Wang, B., and LinHo, 2002: Rainy season of the Asian–Pacific summer monsoon. *J. Climate,* **15,** 386–398.

Wu, G. X., and H. Liu, 1998: Vertical vorticity development owing to down-sliding at slantwise isentropic surface. *Dyn. Atmos. Oceans,* **27,** 715–743.

——, and Y. Zhang, 1998: Tibetan Plateau forcing and the timing of the monsoon onset over South Asia and the South China Sea. *Mon. Wea. Rev.,* **126,** 913–927.

——, and Y. Liu, 2003: Summertime quadruplet heating pattern in the subtropics and associated atmospheric circulation. *Geophys. Res. Lett.,* **30,** 1201, doi:10.1029/2002GL016209.

——, ——, and P. Liu, 1999: The effect of spatially nonuniform heating on the formation and variation of subtropical high. Part I: Scale analysis (in Chinese). *Acta Meteor. Sin.,* **57,** 257–263.

——, J. Chou, Y. Liu, and J. He, 2002: *Dynamics of the Formation and Variation in Subtropical Anticyclones* (in Chinese). Science Press, 314 pp.

——, and Coauthors, 2007: The influence of the mechanical and thermal forcing of the Tibetan Plateau on the Asian climate. *J. Hydrometeor.,* **8,** 770–789.

——, Y. Guan, T. Wang, Y. Liu, J. Yan, and J. Mao, 2011: Vortex genesis over the Bay of Bengal in spring and its role in the onset of the Asian Summer Monsoon. *Sci. China Earth Sci.,* **54,** 1–9.

——, ——, Y. Liu, J. Yan, and J. Mao, 2012: Air–sea interaction and formation of the Asian summer monsoon onset vortex over the Bay of Bengal. *Climate Dyn.,* **38,** 261–279.

Xie, S. P., and S. Philander, 1994: A coupled ocean-atmosphere model of relevance to the ITCZ in the eastern Pacific. *Tellus,* **46A,** 340–350.

Yan, J. H., 2005: Asian summer monsoon onset and advancing process and the variation of the subtropical high (in Chinese). Ph.D. dissertation, Graduate University of Chinese Academy of Sciences, 147 pp.

Yanai, M., S. Esbensen, and J.-H. Chu, 1973: Determination of bulk properties of tropical cloud clusters from large-scale heat and moisture budgets. *J. Atmos. Sci.,* **30,** 611–627.

Zhang, H.-M., J. J. Bates, and R. W. Reynolds, 2006: Assessment of composite global sampling: Sea surface wind speed. *Geophys. Res. Lett.,* **33,** L17714, doi:10.1029/2006GL027086.

Zhang, Q., G. Wu, and Y. Qian, 2002: The bimodality of the 100hPa South Asian high and its relationship to the climate anomaly over East Asia in summer. *J. Meteor. Soc. Japan,* **80,** 733–744.

Zhu, Q. G., J. He, and P. Wang, 1986: A study of circulation differences between East Asian and Indian summer monsoon with their interaction. *Adv. Atmos. Sci.,* **3,** 466–477.